

RECEIVED: June 25, 2024
REVISED: November 10, 2024
ACCEPTED: December 18, 2024
PUBLISHED: January 28, 2025

Plasma constraints on the millicharged dark matter

Mikhail V. Medvedev^{id}^{a,b,c,d,e} and Abraham Loeb^a

^a*Department of Astronomy, Harvard University,
Cambridge, MA 02138, U.S.A.*

^b*Institute for Advanced Study, School for Natural Sciences,
Princeton, NJ 08540, U.S.A.*

^c*Department of Astrophysical Sciences, Princeton University,
Princeton, NJ 08544, U.S.A.*

^d*Department of Physics and Astronomy, University of Kansas,
Lawrence, KS 66045, U.S.A.*

^e*Laboratory for Nuclear Science, Massachusetts Institute of Technology,
Cambridge, MA 02139, U.S.A.*

E-mail: medvedev@ku.edu, aloeb@cfa.harvard.edu

ABSTRACT: Dark matter particles were suggested to have an electric charge smaller than the elementary charge unit e . The behavior of such a medium is similar to a collisionless plasma. In this paper, we set new stringent constraints on the charge and mass of the millicharged dark matter particle based on observational data on the Bullet X-ray Cluster.

KEYWORDS: dark matter theory, extragalactic magnetic fields

ARXIV EPRINT: [2406.15750](https://arxiv.org/abs/2406.15750)

Contents

1	Introduction	1
2	Bullet Cluster constraints	1
3	Discussion	5

1 Introduction

Millicharged particles with the electric charge being smaller than the unit (electron) charge, i.e., $q_\chi = \epsilon e$ with $\epsilon < 1$, is a possible theoretical extension of the standard model of particle physics. Hereafter, we denote the charge magnitude by q_χ , whereas individual particles can have both positive and negative charges to satisfy global charge neutrality of the medium. This possibility has been discussed extensively recently and there are numerous searches that constrain the charge-to-mass ratio of such particles, see e.g., refs. [1–3]. The compilation of the exclusion regions is presented in figure 1. The regions based on experimental data are labeled as follows. “ ${}^9\text{Be}^+$ ” labels the constraint from the Paul trap experiment [4], “ ${}^{40}\text{Ca}^+$ ” refers to the Penning trap experiment [5], “antiproton” refers to the cryogenic Penning trap [6], “collider” represents the combined limits set by collider experiments, e.g., SLAC and LEP [7, 8], “Xenon” denotes the limit from Xenon100 experiment [9].

The 21-cm temperature anomaly reported by the EDGES Collaboration [10] received much attention and has been interpreted as a result of the interaction of baryons with millicharged dark matter [11, 12]. The allowed region is marked in white in figure 1 and labeled “ T_{21} ”. Such an interpretation has been ruled out based on astrophysical observations. The constraints include the limit on the dark-matter-baryon interaction using the CMB Planck15 data labeled “Planck” [13], the implications from the light element abundances produced by Big Bang nucleosynthesis, labeled “ ΔN_{eff} ” [14], and the limit derived from observations of the nearby 1987A supernova, labeled “SN1987A” [15].

Despite numerous existing constraints, the possibility that the dark matter can be composed of millicharged particles is not ruled out as of yet. In this paper, we present new stringent cosmological constraints based on observations of the Bullet X-ray Cluster.

2 Bullet Cluster constraints

The Bullet X-ray Cluster 1E 0657-56 consists of two colliding sub-clusters and provides a strong indication for the existence of dark matter which is not coupled to the baryons. Indeed, the positions of the clumps of two collisionless components — dark matter and stars — do not coincide with the position of the collisional hot intracluster gas [16–19]. The separation of the two mass centroids is about $d_c \sim 0.3$ Mpc. The two sub-clusters collide with a relative velocity in the range $v \sim 3000 - 4500$ km s⁻¹ [20, 21]. We use the value of $v \sim 4000$ km s⁻¹ in our estimates. It is well known that galaxy clusters possess rather strong magnetic fields of a microgauss strength, i.e., sub-equipartition with the gas, $\beta \equiv 4\pi p/B^2 \sim 100$ (with p being

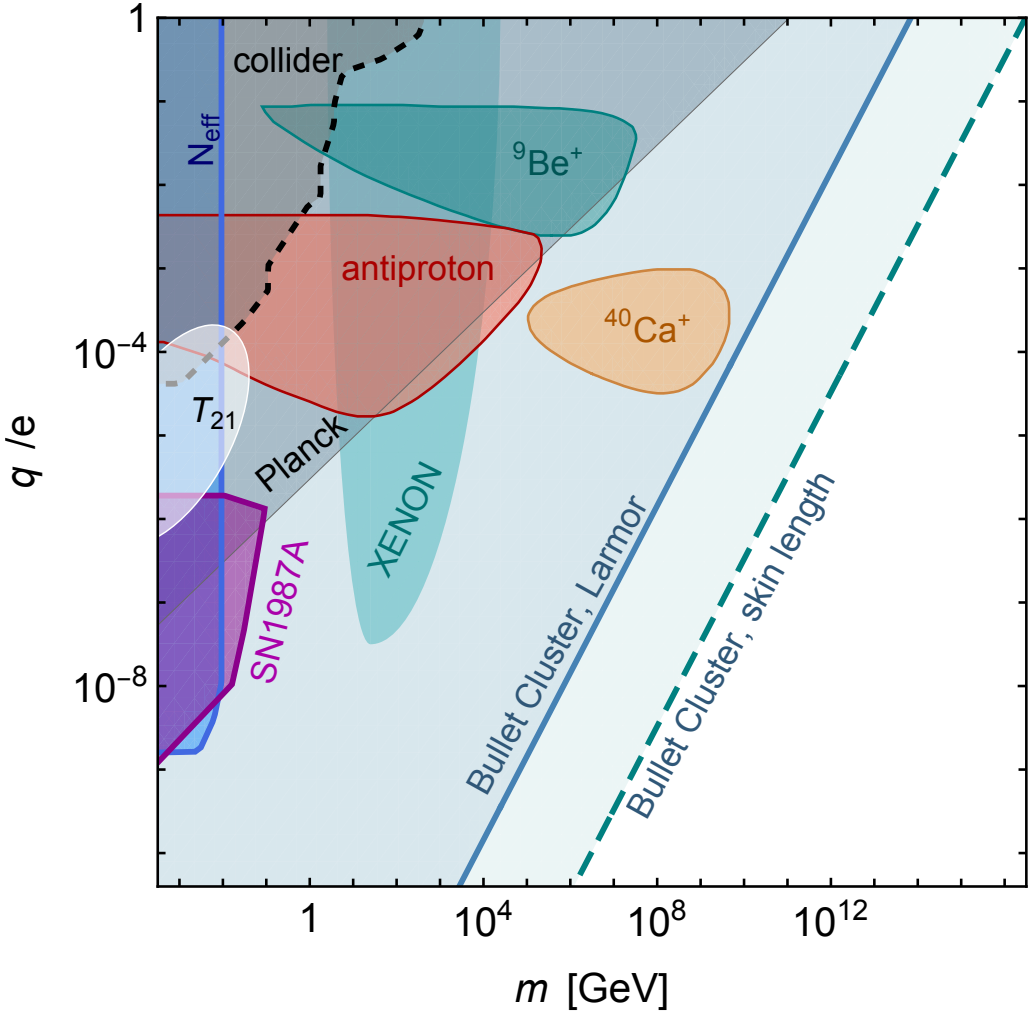


Figure 1. The charge-mass exclusion (shaded) regions for millicharged dark matter. For existing constraints, see text. The two inclined lines (solid and dashed) represent the galaxy cluster constraints discussed in this paper, eqs. (2.2) and (2.5), respectively.

the gas pressure). For instance, Abel 2345 has B-field in the range of $B \simeq 0.3 - 2.8 \mu\text{G}$ [22], which is a factor of three smaller than the equipartition value. The Bullet Cluster radio emission indicates the presence of a strong magnetic field, though its strength is poorly constrained [23, 24]. For our estimates, it is reasonable to assume that $B \sim 1 \mu\text{G}$. This is a factor of a few below the equipartition value [25]. Furthermore, the very low fraction of the polarized emission — of the order of a percent — indicates the absence of a large scale ordered magnetic field. Instead, this is indicative of the turbulent nature of the field.

Now, suppose that dark matter particles, denoted by χ , have a small charge, q_χ . We do not set an *a priori* constraint on the value of the charge, but instead use the observed properties of the Bullet Cluster to draw two constraints on the dark matter electric charge.

First, charged dark matter particles experience the Lorentz force in the intracluster magnetic fields. The characteristic Larmor radius v/ω_B (for a cyclotron frequency ω_B) of

these particles is given by

$$r_L \simeq \frac{v m_\chi c}{q_\chi B} \simeq (4 \times 10^{10} \text{ cm}) (q_\chi/e)^{-1} m_{\chi, \text{GeV}} v_{4000} B_{\mu\text{G}}^{-1}, \quad (2.1)$$

where the velocity v is normalized to 4000 km/s, i.e., $v_{4000} = v/(4000 \text{ km s}^{-1})$, the particle mass is in GeV and the magnetic field is in microgauss. Here we assumed an isotropic particle distribution, so that we can approximately write $\mathbf{v} \times \mathbf{B} \simeq vB$. In a turbulent B-field of a colliding and merging cluster, the Larmor scale is a characteristic distance the charged dark matter can travel ballistically, before their motion is substantially deflected by the Lorentz force. Thus, the distance between the mass centroids must be substantially smaller than the Larmor radius of dark matter particles, $d_c < r_L$. This condition yields the first charge-mass constraint:

$$q_\chi/e \lesssim 5 \times 10^{-14} m_{\chi, \text{GeV}} d_{c, 0.3 \text{Mpc}}^{-1} v_{4000} B_{\mu\text{G}}^{-1}. \quad (2.2)$$

This inequality represents an upper bound on the dark matter millicharge. It is shown in figure 1 and labeled as ‘‘Bullet Cluster, Larmor’’. The shaded region above the line is ruled out.

We should note here that one does not need the small scales in the dark matter map to be well resolved. If the plasma kinetic scale λ_χ is much smaller than the cluster size, than dark matter behaves like gas. In this case, the whole distribution of dark matter and gas should be nearly identical, regardless of the actual value of λ_χ . This is not seen. Thus, for our constraint we are mostly interested in the clumps comparable to the cluster size, so spatial resolution should not be a problem. Also, the typical random velocities of dark matter particles in a cluster are of the order of 1000 km/s, so the millicharged plasma is not cold. However, this value is considerably smaller than the direct velocity of 4000 km/s. Hence, we neglect this an order unity uncertainty in our order of magnitude estimate. Finally, the cluster magnetic field is too weak to be dynamically important. Nevertheless, being ‘‘frozen in plasma’’, the magnetic field transfers momentum through plasma, between the colliding millicharged plasma blobs. The massive collision between dark matter-dominated sub-clusters can stretch the magnetic field lines along the direction of the collision, make them open and modified. The reader is referred to refs. [26–28] for more details. Under these conditions the trapping of millicharged dark matter considered in our estimate may be modified. The above collision process is rather complicated, so dedicated numerical simulations are desirable.

Second, millicharged dark matter forms a collisionless plasma throughout the universe, with a small charge-to-mass ratio. When plasma blobs collide, e.g., as in the Bullet Cluster, their plasma is susceptible to various instabilities, both kinetic and magnetohydrodynamic. The fastest ones (and most important here) are the kinetic instabilities, such as the Weibel, Buneman and two-stream instabilities. Given that kinetic energy associated with dark matter greatly exceeds that of other constituents (e.g., magnetized baryonic gas), these instabilities should be robustly excited through dark matter interactions. The kinetic plasma instabilities typically operate on the so called ‘‘plasma time scale’’, $\tau_{p,\chi} \simeq \omega_{p,\chi}^{-1}$ where the

plasma frequency of species χ is

$$\begin{aligned}\omega_{p,\chi} &= \left(4\pi q_\chi^2 n_\chi / m_\chi\right)^{1/2} \\ &\simeq (3 \times 10^2 \text{ s}) (q_\chi/e) m_{\chi,\text{GeV}}^{-1} \delta_{c,4}^{1/2},\end{aligned}\quad (2.3)$$

where $n_\chi = \delta_c \rho_{\text{crit}} / m_\chi$ is the intra-cluster millicharged dark matter density, $\rho_{\text{crit}} \simeq 10^{-29} \text{ g cm}^{-3}$ is the critical density of the universe, $\delta_{c,4} = \delta_c / 10^4$, and δ_c is the cluster overdensity, characterizing how much the density of dark matter within the cluster exceeds the critical density. The value of $\delta_c \sim 10^4$ is a lower limit on the density of interest in the core of the Bullet Cluster. The estimate for the value of δ_c follows from the gravitational lensing map of the Bullet Cluster [19], which yields the dark matter density of about $2 \times 10^{-25} \text{ g cm}^{-3}$ within about 0.3 Mpc of its center, which corresponds to $\delta_c \sim 2 \times 10^4$.

These instabilities result in density and field inhomogeneities on kinetic scales. The Weibel instability produces filaments and associated magnetic fields elongated along the plasma motion. In contrast, the Buneman and two-stream instabilities cause plasma bunching (mediated by electric fields) into planar fronts perpendicular to the plasma motion. To understand how these processes set in and operate in the colliding cluster environment would require dedicated numerical simulations. A simple but robust estimate can, however, be made as follows.

The general outcome of the kinetic instabilities driven by cluster collision is the formation of density fluctuations and inhomogeneities of the millicharged dark matter in the region of halo interaction. The characteristic scale of these inhomogeneities is the so-called “*plasma skin length*”,

$$\begin{aligned}\lambda_\chi &\simeq c / \omega_{p,\chi} \\ &\simeq (10^8 \text{ cm}) (q_\chi/e)^{-1} m_{\chi,\text{GeV}} \delta_{c,4}^{-1/2}.\end{aligned}\quad (2.4)$$

From an observational perspective, the absence of large dark matter inhomogeneities in gravitational lensing maps on scales of order the mass centroid separation implies that the plasma skin length is comparable or exceeds this separation, namely $\lambda_\chi \gtrsim d_c$. This condition sets the second charge-mass constraint:

$$q_\chi/e \lesssim 10^{-16} m_{\chi,\text{GeV}} d_{c,0.3\text{Mpc}}^{-1} \delta_{c,4}^{-1/2}.\quad (2.5)$$

This constraint is depicted in figure 1 by the dashed line, labeled as “Bullet Cluster, skin length”. The shaded region above (and to the left of) the line is ruled out. Note that this second constraint is independent of the magnetic field, but depends on the dark matter over-density parameter instead.

We should stress here that the effect of gravity has been neglected in the presented estimate. It is very desirable to perform dedicated numerical or analytical studies of how the above plasma instabilities are modified by self-gravity. We are not aware of such studies at present. One can, however, theoretically speculate about a possible effect. Self-gravity introduces a second scale in the problem — the Jeans scale, l_J . At scales above it, one expects Jeans instability leading to the gravitational collapse to dominate whereas at much smaller

scales, gravity is subdominant to other effects and can generally be ignored. In the case at hand, the Jeans scale is not expected to be too small compared to the cluster size itself $l_J \gtrsim d_c$, otherwise it would gravitationally fragment. Therefore, the kinetic scales can only be marginally affected by self-gravity when all the scales are comparable $\lambda_\chi \sim d_c \sim l_J$ (much smaller λ_χ 's are unaffected). Yet, even if it is so, self-gravity would enhance the kinetically produced clumps via subsequent gravitational collapse (provided there is enough time), thus enhancing the density contrast, and hence observational visibility of these clumps. Thus, inclusion of self-gravity generally strengthens our estimate. We reiterate that a dedicated study of this problem is highly desirable.

3 Discussion

We derived two robust constraints on millicharged dark matter properties based on observations of the Bullet X-ray Cluster. The first constraint is set by the fact that the mass density centroid separation cannot exceed the Larmor radius of the millicharged dark matter particles. The second constraint follows from that fact that dark matter density inhomogeneities could form via collisionless kinetic instabilities excited by the collision of the two sub-clusters. The absence of substantial inhomogeneities in gravitational lensing maps on scales smaller than the mass centroid separation puts the lower limit on the millicharged plasma skin length. These constraints are given by eqs. (2.2) and (2.5), and shown in figure 1. Interestingly, despite the different physics involved, both constraints appear very similar in that they constrain the charge-to-mass ratio, q_χ/m_χ .

Although this study is motivated by the millicharged dark matter model in which the charge is smaller than the electron charge ($q_\chi < e$), the constraints can be used for *any* set of particles with a charge q_χ . For example, the constraints obtained here allow for the dark matter to be multiply charged, $q_\chi > e$, provided the particles are very massive, $m_\chi > 10^{16}$ GeV. These include charged primordial black holes. For a typical mass of $m_{\text{bh}} \sim 10^{17}$ g $\simeq 10^{41}$ GeV, the charge is constrained to be below $q_{\text{bh}} \lesssim 10^{25}e$. Apparently, this is not a strong constraint on the primordial black hole charge.

The charge attained by a black hole, immersed in the hot ionized gas medium, can be estimated as follows. First, a black hole in the membrane paradigm can be considered as a conducting sphere. Second, a conductor immersed in an ionized gas of temperature T attains a floating potential, $V \simeq k_B T/e \sim 10^{-7}T$, where the temperature is in Kelvin and the potential is in Volts. A sphere of charge Q and radius r produces an electric potential $V = Q/r = k_B T/e$. The black hole's Schwarzschild radius is $r_{\text{bh}} = 2Gm_{\text{bh}}/c^2 \sim 10^{-28}m_{\text{bh}}$ in cgs units. For $m_{\text{bh}} \sim 10^{17}$ g, its radius is a hundred proton radii, $r_{\text{bh}} \sim 10^{-11}$ cm. Therefore, we estimate the charge as

$$q_{\text{bh}} \sim \frac{2Gk_B}{ec^2} T m_{\text{bh}} \sim (0.8e) T_{8.3} m_{\text{bh},17}, \quad (3.1)$$

where in the second equality the charge is expressed in the units of an elementary charge, m_{bh} is normalized to 10^{17} g, and T is normalized to 2×10^8 K (i.e., $T_{8.3} = T/10^{8.3}$ K) which corresponds to the Bullet Cluster gas temperature of about 17.4 keV [29]. Thus, we see that a typical charge of a primordial black hole immersed in a hot ionized ambient gas is many orders of magnitude smaller than the limit set by the Bullet Cluster data.

Acknowledgments

This work is supported by NSF grants PHY-2010109 and PHY-2409249.

References

- [1] E. Izaguirre and I. Yavin, *New window to millicharged particles at the LHC*, *Phys. Rev. D* **92** (2015) 035014 [[arXiv:1506.04760](https://arxiv.org/abs/1506.04760)] [[INSPIRE](#)].
- [2] A. Berlin, D. Hooper, G. Krnjaic and S.D. McDermott, *Severely Constraining Dark Matter Interpretations of the 21-cm Anomaly*, *Phys. Rev. Lett.* **121** (2018) 011102 [[arXiv:1803.02804](https://arxiv.org/abs/1803.02804)] [[INSPIRE](#)].
- [3] D. Budker et al., *Millicharged Dark Matter Detection with Ion Traps*, *PRX Quantum* **3** (2022) 010330 [[arXiv:2108.05283](https://arxiv.org/abs/2108.05283)] [[INSPIRE](#)].
- [4] D.A. Hite et al., *100-Fold Reduction of Electric-Field Noise in an Ion Trap Cleaned with In Situ Argon-Ion-Beam Bombardment*, *Phys. Rev. Lett.* **109** (2012) 103001 [[arXiv:1112.5419](https://arxiv.org/abs/1112.5419)].
- [5] J.F. Goodwin, G. Stutter, R.C. Thompson and D.M. Segal, *Resolved-Sideband Laser Cooling in a Penning Trap*, *Phys. Rev. Lett.* **116** (2016) 143002.
- [6] M.J. Borchert et al., *Measurement of Ultralow Heating Rates of a Single Antiproton in a Cryogenic Penning Trap*, *Phys. Rev. Lett.* **122** (2019) 043201 [[arXiv:1901.09860](https://arxiv.org/abs/1901.09860)] [[INSPIRE](#)].
- [7] A.A. Prinz et al., *Search for millicharged particles at SLAC*, *Phys. Rev. Lett.* **81** (1998) 1175 [[hep-ex/9804008](https://arxiv.org/abs/hep-ex/9804008)] [[INSPIRE](#)].
- [8] G. Marocco and S. Sarkar, *Blast from the past: Constraints on the dark sector from the BEBC WA66 beam dump experiment*, *SciPost Phys.* **10** (2021) 043 [[arXiv:2011.08153](https://arxiv.org/abs/2011.08153)] [[INSPIRE](#)].
- [9] J.M. Cline, Z. Liu and W. Xue, *Millicharged Atomic Dark Matter*, *Phys. Rev. D* **85** (2012) 101302 [[arXiv:1201.4858](https://arxiv.org/abs/1201.4858)] [[INSPIRE](#)].
- [10] J.D. Bowman et al., *An absorption profile centred at 78 megahertz in the sky-averaged spectrum*, *Nature* **555** (2018) 67 [[arXiv:1810.05912](https://arxiv.org/abs/1810.05912)] [[INSPIRE](#)].
- [11] R. Barkana, *Possible interaction between baryons and dark-matter particles revealed by the first stars*, *Nature* **555** (2018) 71 [[arXiv:1803.06698](https://arxiv.org/abs/1803.06698)] [[INSPIRE](#)].
- [12] A. Aboubrahim, P. Nath and Z.-Y. Wang, *A cosmologically consistent millicharged dark matter solution to the EDGES anomaly of possible string theory origin*, *JHEP* **12** (2021) 148 [[arXiv:2108.05819](https://arxiv.org/abs/2108.05819)] [[INSPIRE](#)].
- [13] K.K. Boddy et al., *Critical assessment of CMB limits on dark matter-baryon scattering: New treatment of the relative bulk velocity*, *Phys. Rev. D* **98** (2018) 123506 [[arXiv:1808.00001](https://arxiv.org/abs/1808.00001)] [[INSPIRE](#)].
- [14] C. Boehm, M.J. Dolan and C. McCabe, *A Lower Bound on the Mass of Cold Thermal Dark Matter from Planck*, *JCAP* **08** (2013) 041 [[arXiv:1303.6270](https://arxiv.org/abs/1303.6270)] [[INSPIRE](#)].
- [15] J.H. Chang, R. Essig and S.D. McDermott, *Supernova 1987A Constraints on Sub-GeV Dark Sectors, Millicharged Particles, the QCD Axion, and an Axion-like Particle*, *JHEP* **09** (2018) 051 [[arXiv:1803.00993](https://arxiv.org/abs/1803.00993)] [[INSPIRE](#)].
- [16] D. Clowe, A. Gonzalez and M. Markevitch, *Weak lensing mass reconstruction of the interacting cluster 1E 0657-558: Direct evidence for the existence of dark matter*, *Astrophys. J.* **604** (2004) 596 [[astro-ph/0312273](https://arxiv.org/abs/astro-ph/0312273)] [[INSPIRE](#)].

- [17] M. Markevitch et al., *Direct constraints on the dark matter self-interaction cross-section from the merging galaxy cluster 1E 0657-56*, *Astrophys. J.* **606** (2004) 819 [[astro-ph/0309303](#)] [[INSPIRE](#)].
- [18] D. Clowe et al., *A direct empirical proof of the existence of dark matter*, *Astrophys. J. Lett.* **648** (2006) L109 [[astro-ph/0608407](#)] [[INSPIRE](#)].
- [19] D. Paraficz et al., *The bullet cluster at its best: weighing stars, gas, and dark matter*, *Astron. Astrophys.* **594** (2016) A121 [[arXiv:1209.0384](#)] [[INSPIRE](#)].
- [20] R. Thompson, R. Davé and K. Nagamine, *The rise and fall of a challenger: the Bullet Cluster in Λ cold dark matter simulations*, *Mon. Not. Roy. Astron. Soc.* **452** (2015) 3030 [[arXiv:1410.7438](#)] [[INSPIRE](#)].
- [21] E. Hayashi and S.D.M. White, *How Rare is the Bullet Cluster?*, *Mon. Not. Roy. Astron. Soc.* **370** (2006) L38 [[astro-ph/0604443](#)] [[INSPIRE](#)].
- [22] C. Stuardi et al., *The intracluster magnetic field in the double relic galaxy cluster Abell 2345*, *Mon. Not. Roy. Astron. Soc.* **502** (2021) 2518 [[arXiv:2101.09302](#)] [[INSPIRE](#)].
- [23] T.W. Shimwell et al., *Deep radio observations of the radio halo of the bullet cluster 1E 0657-55.8*, *Mon. Not. Roy. Astron. Soc.* **440** (2014) 2901 [[arXiv:1403.2393](#)] [[INSPIRE](#)].
- [24] S.P. Sikhosana et al., *MeerKAT’s view of the bullet cluster 1E 0657-55.8*, *Mon. Not. Roy. Astron. Soc.* **518** (2022) 4595 [[arXiv:2207.05492](#)].
- [25] S. Paul et al., ‘*Rings*’ of diffuse radio emission surrounding the Bullet cluster, [arXiv:1804.02588](#) [[INSPIRE](#)].
- [26] G. Brunetti and T.W. Jones, *Cosmic rays in galaxy clusters and their nonthermal emission*, *Int. J. Mod. Phys. D* **23** (2014) 1430007 [[arXiv:1401.7519](#)] [[INSPIRE](#)].
- [27] R.J. van Weeren et al., *Diffuse Radio Emission from Galaxy Clusters*, *Space Sci. Rev.* **215** (2019) 16 [[arXiv:1901.04496](#)] [[INSPIRE](#)].
- [28] Y. Hu et al., *Synchrotron intensity gradient revealing magnetic fields in galaxy clusters*, *Nature Commun.* **15** (2024) 1006 [[arXiv:2306.10011](#)] [[INSPIRE](#)].
- [29] W. Tucker et al., *1E 0657-56: A Contender for the Hottest Known Cluster of Galaxies*, *Astrophys. J. Lett.* **496** (1998) L5 [[astro-ph/9801120](#)] [[INSPIRE](#)].